Icarus 305 (2018) 80–83

Contents lists available at ScienceDirect

Icarus

journal homepage: www.elsevier.com/locate/icarus

Corrigendum

Corrigendum to “Interpreting the librations of a synchronous satellite – How their phase assesses Mimas’ global ocean” [Icarus 282 (2017) 276–289]

Benoît Noyelles

NAmur Center for CompleX SYStems (NAXYS), University of Namur, Rempart de la Vierge 8, Namur, B-5000, Belgium

Abstract

A mistake appeared in the original paper, which propagated. This affects the phase of the diurnal libration. The conclusions are unchanged.

Keywords

Resonances; Spin-orbit – Rotational dynamics – Satellites; Shapes – Celestial mechanics – Saturn; Satellites.

An error appeared in the derivation of a formula, which propagated and altered the expression for the diurnal and semi-diurnal librations. The formulae and figures associated are to be replaced by the following ones. The conclusions of the paper are unchanged.

In Section 4, the Eq. (35) should now read

$$\Gamma = \left(\frac{2}{5}MR^2 + \frac{M_\saturn R^5}{a^3}\left(k_f\left(\frac{5}{9}+\frac{1}{2}e^2\right) + ek_2(\nu_1)\cos\mathcal{M} + \frac{3}{2}e^2k_2(\nu_2)\cos 2\mathcal{M}\right)\right)\ddot{\sigma}$$
$$-\frac{M_\saturn R^5}{a^3}(n-\dot{\varpi})\left(k_2(\nu_1)e\sin\mathcal{M} + 3k_2(\nu_2)e^2\sin 2\mathcal{M}\right)(n+\dot{\sigma}), \tag{1}$$

which gives (Eq. (41) and (42))

$$K_5 = 6en^2\frac{M_\saturn R^5}{a^3}\left(k_f - \frac{5}{6}k_2(\nu_1)\right), \tag{2}$$

$$K_6 = \frac{51}{4}e^2n^2\frac{M_\saturn R^5}{a^3}\left(k_f - \frac{13}{17}k_2(\nu_2)\right), \tag{3}$$

and (Eq. (50))

$$\kappa_1 = 6en^2\frac{(I_{22}-I_{11})^{(f)} + M_\saturn\frac{R^5}{a^3}\left(k_f - \frac{5}{6}k_2(\nu_1)\right)}{\frac{2}{5}MR^2 + k_f\left(\frac{5}{9}+\frac{e^2}{2}\right)M_\saturn\frac{R^5}{a^3}}, \tag{4}$$

and the new Table 4 (See Table 1):

In the Section 7.1, the Eq. (79) becomes

DOI of original article: 10.1016/j.icarus.2016.10.001

E-mail address: benoit.noyelles@unamur.be

https://doi.org/10.1016/j.icarus.2018.01.005

0019-1035

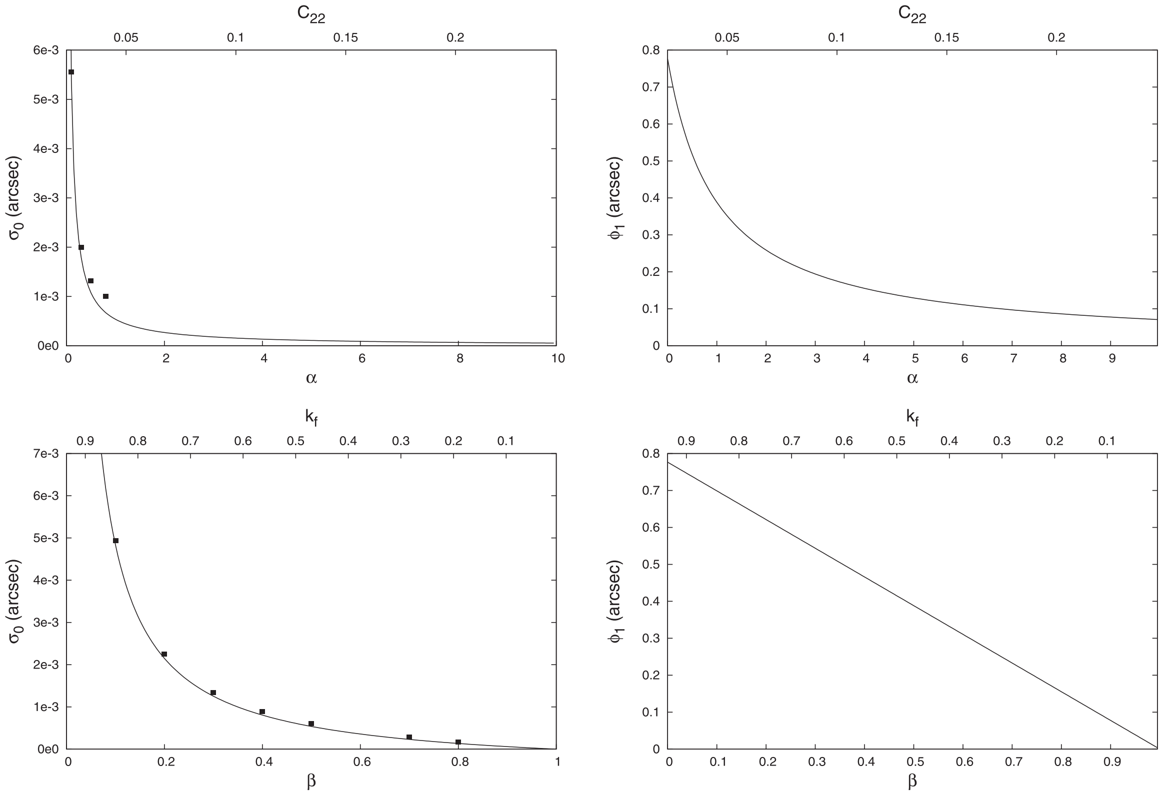

Fig. 1. (Figure 8) Rotational quantities for Epimetheus in the dissipative case, for $k_f = 1.5$ (top), and $C_{22} = 1.426 \times 10^{-2}$ (down). The lines come from the analytical formulae, while the squares result from numerical simulations.

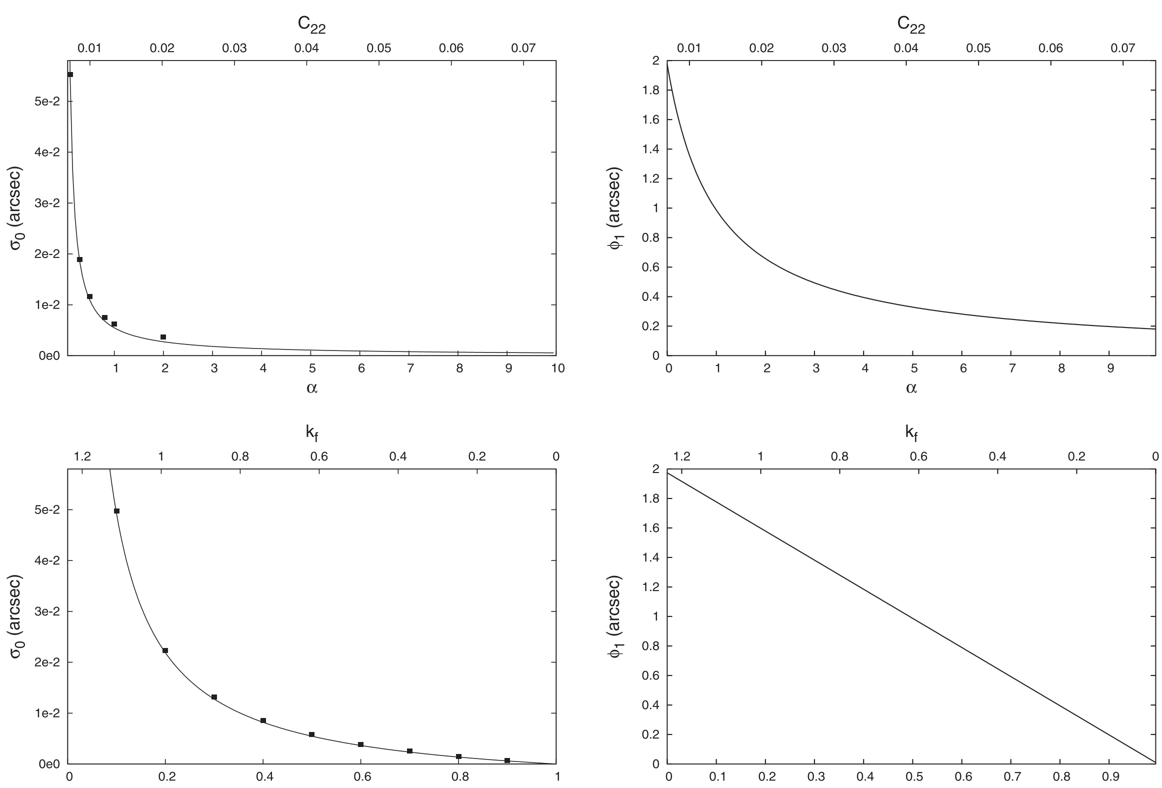

Fig. 2. (Figure 9) Rotational quantities for Mimas in the dissipative case, for $k_f = 1.5$ (top), and $C_{22} = 5.606 \times 10^{-3}$ (down). The lines come from the analytical formulae, while the squares result from numerical simulations.

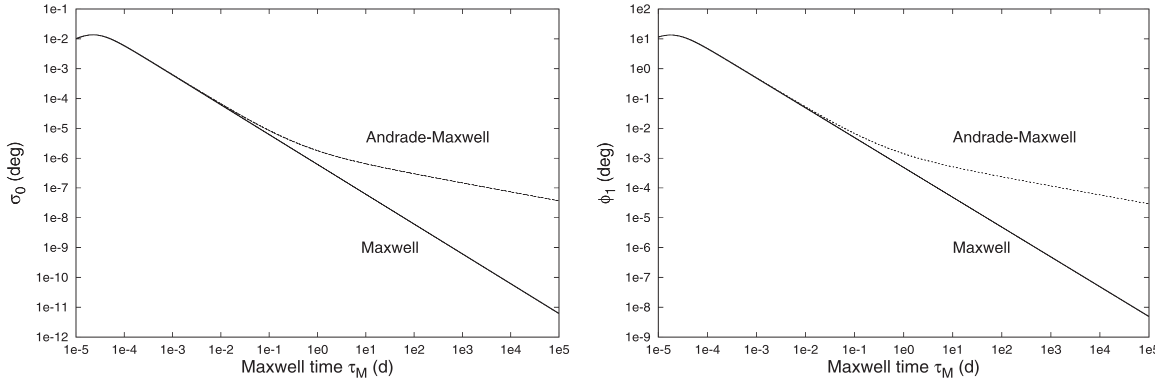

Fig. 3. (Figure 11) Influence of the rheology on the rotation of Epimetheus, for $\alpha = 1.21$. The Andrade–Maxwell model has been applied with $N = 0.3$, this parameter influencing the slope for high Maxwell times.

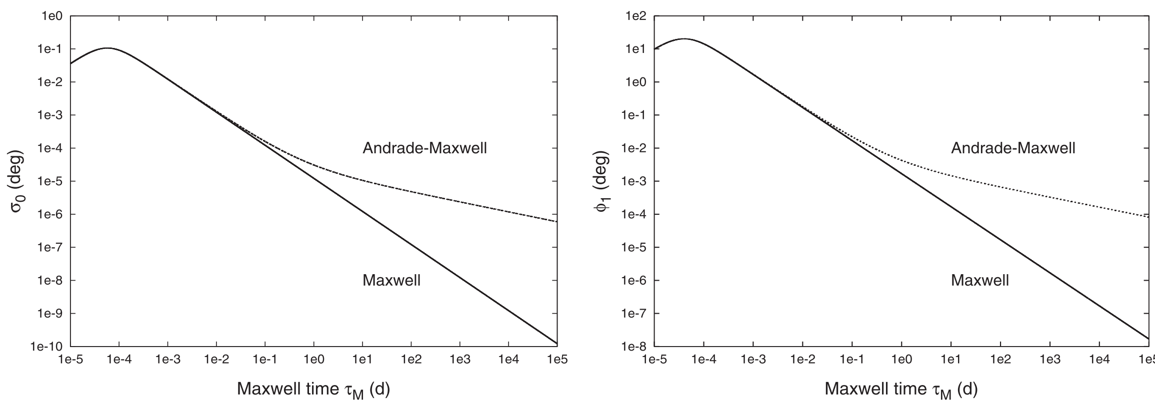

Fig. 4. (Figure 12) Influence of the rheology on the rotation of Mimas, for $\alpha = 0.6225$, and $N = 0.3$.

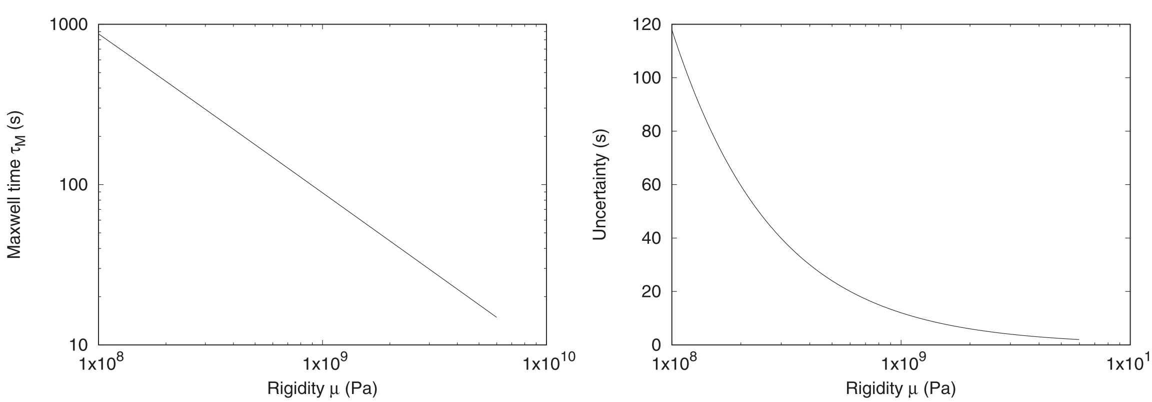

Fig. 5. (Figure 13) Maxwell times of Mimas deduced from the diurnal phase shift ϕ_1 (left), and the uncertainty associated (right). These numbers are much shorter than expected from our knowledge of Mimas.

$$\Gamma = \left(\frac{2}{5}MR^2 + \frac{M_{♄}R^5}{a^3}\left(k_f\left(\frac{5}{9}+\frac{1}{2}e^2\right) + ek_2(\nu_1)\cos\mathcal{M} + \frac{3}{2}e^2k_2(\nu_2)\cos 2\mathcal{M}\right)\right.$$
$$\left. + e\left(\frac{k_2}{Q}\right)(\nu_1)\sin\mathcal{M} + \frac{3}{2}e^2\left(\frac{k_2}{Q}\right)(\nu_2)\sin 2\mathcal{M}\right)\ddot{\sigma}$$
$$-\frac{M_{♄}R^5}{a^3}(n-\dot{\varpi})\Big(k_2(\nu_1)e\sin\mathcal{M} + 3k_2(\nu_2)e^2\sin 2\mathcal{M}$$
$$-\left(\frac{k_2}{Q}\right)(\nu_1)e\cos\mathcal{M} - 3\left(\frac{k_2}{Q}\right)(\nu_2)e^2\cos 2\mathcal{M}\Big)(\dot{\sigma}+n), \quad (5)$$

and gives the followings Eqs. (82) & (83):

$$K_{12} = 5en^2\frac{M_{♄}R^5}{a^3}\left(\frac{k_2}{Q}\right)(\nu_1), \quad (6)$$

Table 1
(Table 4) Comparison with previous studies. The formulae labeled *This study* are given by the Eq. (49) and (50), but there expansion is here limited to the degree 1 in the eccentricity.

	Van Hoolst et al. (2013)	Richard et al. (2014)	This study
ω_0^2	$3n^2\frac{B-A}{C}\left(1-\frac{k_2}{k_f}\right)$	$3n^2\frac{B-A}{C}$	$3n^2\frac{(I_{22}-I_{11})^{(f)}}{\frac{2}{5}MR^2+\frac{5}{9}k_f M_{♄}\frac{R^5}{a^3}}$
κ_1	$6en^2\frac{B-A}{C}\left(1-\frac{5}{6}\frac{k_2}{k_f}\right)$	$6en^2\left(\frac{B-A}{C}-\frac{h_2}{2}M_{♄}\frac{R^5}{Ca^3}\right)$	$6en^2\frac{(I_{22}-I_{11})^{(f)}+M_{♄}\frac{R^5}{a^3}\left(k_f-\frac{5}{6}k_2(\nu_1)\right)}{\frac{2}{5}MR^2+\frac{5}{9}k_f M_{♄}\frac{R^5}{a^3}}$

$$K_{13} = \frac{39}{4}e^2n^2\frac{M_{♄}R^5}{a^3}\left(\frac{k_2}{Q}\right)(\nu_2), \tag{7}$$

while we should have now, in the Section 7.2, the new Eqs. (90) and (95):

$$\kappa_2 = \frac{5eM_{♄}\frac{R^5}{a^3}\left(\frac{k_2}{Q}\right)(\nu_1)}{\frac{2}{5}MR^2+\frac{M_{♄}R^5}{a^3}k_f\left(\frac{5}{9}+\frac{e^2}{2}\right)}, \tag{8}$$

$$\tan\phi_1 = \frac{5}{6}\frac{M_{♄}\frac{R^5}{a^3}\left(\frac{k_2}{Q}\right)(\nu_1)}{(I_{22}-I_{11})^{(f)}+M_{♄}\frac{R^5}{a^3}\left(k_f-\frac{5}{6}k_2(\nu_1)\right)}. \tag{9}$$

The Figs. 8, 9, 11, 12 & 13 (See Figs. 1–5) have to be updated as well, as:

Finally, some sentences of the fourth paragraph of Section 4 should be updated with new numbers: However, Tajeddine et al. (2014) have measured $\phi_1 = 6.35 \pm 0.8^\circ$, which suggests $\tau_M = 22.26^{+3.38}_{-2.64}$ s for a rigidity $\mu = 4$ GPa. A rigidity ten times smaller, i.e. $\mu = 0.4$ GPa, would give $\tau_M = 221^{+34}_{-26}$ s (Fig. 13 (See Fig. 5)). A smaller k_f would give a Maxwell time of the same order of magnitude, since it would be partly counterbalanced by a larger α. For instance, we would have $\alpha = 1.295 \pm 0.033$ and $\tau_M = 15.09^{+2.48}_{-1.98}$ s for a rigidity $\mu = 4$ GPa and $k_f = 1$.

Acknowledgments

I am indebted to Rose–Marie Baland for her careful reading, and the detection of the original mistake in the Eq. (35). This study took benefit from the financial support of the contract Prodex CR90253 from the Belgian Science Policy Office (BELSPO).

References

Richard, A., Rambaux, N., Charnay, B., 2014. Librational response of a deformed 3-layer titan perturbed by non-keplerian orbit and atmospheric couplings. Planss 93–94, 22–34.
Tajeddine, R., Rambaux, N., Lainey, V., Charnoz, S., Richard, A., Rivoldini, A., Noyelles, B., 2014. Constraints on mimas' interior from cassini ISS libration measurements. Science 346, 322–324.
Van Hoolst, T., Baland, R.-M., Trinh, A., 2013. On the librations and tides of large icy satellites. Icarus 226, 299–315.